Piezoelectric transducer parameter selection for exciting a single mode from multiple modes of Lamb waves*

Zhang Hai-Yan(张海燕)† and Yu Jian-Bo(于建波)

School of Communication and Information Engineering,
Key Laboratory of Specialty Fiber Optics and Optical Access Networks, Shanghai University, Shanghai 200072, *China*

(Received 28 March 2011; revised manuscript received 15 April 2011)

Excitation and propagation of Lamb waves by using rectangular and circular piezoelectric transducers surface-bonded to an isotropic plate are investigated in this work. Analytical stain wave solutions are derived for the two transducer shapes, giving the responses of these transducers in Lamb wave fields. The analytical study is supported by a numerical simulation using the finite element method. Symmetric and antisymmetric components in the wave propagation responses are inspected in detail with respect to test parameters such as the transducer geometry, the length and the excitation frequency. By placing only one piezoelectric transducer on the top or the bottom surface of the plate and weakening the strength of one mode while enhancing the strength of the other modes to find the centre frequency, with which the peak wave amplitude ratio between the S0 and A0 modes is maximum, a single mode excitation from the multiple modes of the Lamb waves can be achieved approximately. Experimental data are presented to show the validity of the analyses. The results are used to optimize the Lamb wave detection system.

Keywords: Lamb waves, parameter selection, analytical stain wave solutions, single mode

PACS: 43.20.+g, 43.35.+d, 47.35.Rs **DOI:** 10.1088/1674-1056/20/9/094301

1. Introduction

Lamb waves, which are elastic guided waves propagating in a solid or on a layer surface with free boundaries, have been widely employed to damage detection.[1] The propagation of the Lamb waves in such structures is a complex process. Multiple modes and their dispersive characteristic make it very difficult to interpret the waveforms, which brings great difficulty to subsequent signal processing and analysis. Therefore, how to use an appropriate signal to reduce the difficulty of the subsequent signal processing is an important issue for the use of Lamb waves in non-destructive testing.[2−7]

For in situ structural health monitoring (SHM) using the nondestructive Lamb wave method, the most common wedge transducers, comb transducers and electromagnetic acoustic transducers (EMATs) are not compact enough to be permanently installed on the structures.[8] Piezoelectric transducers (PZTs) are often used for the generation and the reception of Lamb waves for in situ SHM studies, because they are compact, small, light and cheap. These inexpensive transducers are available in the form of thin piezoceramic wafers that can be surface attached to the detecting structures.[9] Among the various shapes of piezoelctric wafer transducers, rectangular and circular transducers are most commonly used in Lamb wave SHM. The theory of Lamb wave excitation using two shaped piezoelectric transducers as well as the propagation of a Lamb wave in a thin plate is a current research topic.[8,10−13] Lin and Yuan[10] used PZT ceramic disks mounted on an aluminum plate acting as both actuators and sensors to generate and collect A0-mode Lamb waves. The Mindlin plate theory was adopted to model the propagating waves taking both the transverse shear and the rotary inertia effects into account. An analytical expression for the sensor output voltage in terms of the given input excitation signal was derived and experimental work was performed

*Project supported by the National Natural Science Foundation of China (Grant Nos. 11074164 and 10874110), the Shanghai Leading Academic Discipline Project, China (Grant No. S30108), the Science and Technology Commission of Shanghai Municipality, China (Grant No. 08DZ2231100), and the Innovation Foundation of Shanghai Municipal Commission of Education, China (Grant No. 11YZ17).

†Corresponding author. E-mail: hyzh@shu.edu.cn

© 2011 Chinese Physical Society and IOP Publishing Ltd

to verify the accuracy of the analytical model. Experimental results showed that single-mode Lamb waves in the plate could be successfully generated and collected through integrated PZT disks. Xu and Giurgiutiu,[11] Yu *et al.*,[8] and Santoni *et al.*[12] presented analytical and experimental investigations of Lamb wave mode tuning with square and round piezoelectric wafer active sensors (PWASs), showing that the capability to excite only one desired Lamb wave mode was critical for practical SHM applications such as the PWAS phased array technique and the time reversal process (TRP). Santoni *et al.*[12] found that the 300 kHz frequency was optimal for crack detection in a 1 mm-thick aluminum plate using a PWAS array composed of eight 7 mm-square PZTs and the 30 kHz tuning of the A0 Lamb wave mode with a 16-count smoothed tone burst led to the complete elimination of the side wave packets. Wang *et al.*[13] outlined the analytical formulation for the Lamb wave propagation of a narrow-strip beam excited and sensed by piezoelectric transducers, and they analysed in detail the antisymmetric and the symmetric contents of the wave propagation response to system parameters such as the number of cycles and the sensor length. That research provided the mechanistic basis for robust damage detection using data processing.

The aforementioned studies display that the combination of the Lamb wave approach and piezoelectric transducers can offer an alternative damage detection system, which can optionally excite pure symmetric modes, pure antisymmetric modes and the two hybrid modes. On account of the current common rectangular and circle piezoelectric transducers, in this paper, we investigate their excitation in thin plates and the propagation characteristics of the Lamb waves. First, the strain wave analytical solutions of the two types of sensor responses are derived respectively and a finite element numerical calculation is performed to verify the validity of the analytical solutions. Then, symmetric and antisymmetric components in the wave propagation response are inspected in detail with respect to the testing parameters involved, such as the transducer geometry, the length and the excitation frequency. This research provides a theoretical basis for optimizing parameters of the Lamb wave detection system. Finally, experimental results establishing the validity of the analyses are discussed.

2. Theoretical model

We consider two actuators that are symmetrically bonded onto the top and bottom surfaces of the plate by an ideal bond layer that is sufficiently thin and sufficiently stiff. Performance parameters of the two actuators are the same. For the two different shapes of PZTs commonly used in the Lamb wave SHM, namely rectangular and circle, the strain wave solutions of the Lamb waves propagating in the thin plate are different. Here, we first derive the strain wave solution in the case of the rectangular PZT excitation. The structural set up and the coordinate system are as shown in Fig. 1, where the x and the z axes are assumed to be parallel and normal to the wave propagation direction, respectively, and the origin of the coordinate system is located at the median plane.

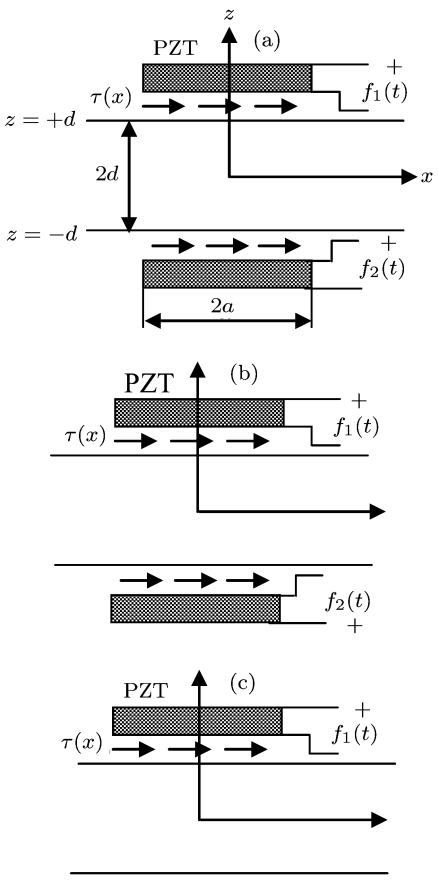


Fig. 1. Schematic PZT layouts for producing different Lamb wave modes include (a) for pure antisymmetric modes, (b) for pure symmetric modes, and (c) for antisymmetric and symmetric hybrid modes.

The boundary conditions under the action of the piezoelectric actuators can be expressed as

$$\begin{cases} \sigma_{zz}|_{z=\pm d} = 0, & |x| < \infty, \\ \sigma_{zx}|_{z=d} = \tau(x) f_1(t), & |x| < a, \\ \sigma_{zx}|_{z=-d} = \tau(x) f_2(t), & |x| < a, \end{cases} \tag{1}$$

where $\tau(x) = a\tau_0 [\delta(x-a) - \delta(x+a)]$ is the shear stress distribution induced by the top or the bottom actuators with a unit voltage input, a is half of the actuator length, d is the plate half thickness, τ_0 is related to the geometric parameters and the material properties of the actuator, the plate and the bond layer, $\delta(x)$ is the Dirac function, $f_1(t)$ and $f_2(t)$ are the transient voltage excitation signals applied to the top and the bottom actuators, respectively.

The mechanical problem of the Lamb wave excitation, propagation and sensing can be considered as the plain strain problem. For the plain strain problem, we have the following wave equations

$$\begin{aligned} &\frac{\partial^2 \varphi}{\partial x^2} + \frac{\partial^2 \varphi}{\partial z^2} + \frac{\omega^2}{c_{\rm l}^2}\varphi = 0, \\ &\frac{\partial^2 \psi}{\partial x^2} + \frac{\partial^2 \psi}{\partial z^2} + \frac{\omega^2}{c_{\rm t}^2}\psi = 0, \end{aligned} \tag{2}$$

where φ and ψ are potential functions for the longitudinal and the transversal waves, respectively, $c_{\rm l}^2 = (\lambda + 2\mu)/\rho$ and $c_{\rm t}^2 = \mu/\rho$ are the longitudinal and the transversal wave speeds, $\lambda = E\nu/[(1-2\nu)(1+\nu)]$ and $\mu = E/[2(1+\nu)]$ are the Lame constants, E, ν and ρ are the Young's modulus, the Poisson ration and the density of the plate, respectively.

According to boundary condition (1) and wave equation (2), we can obtain the strain wave solution at the upper surface of the plate as

$$\begin{aligned} &\varepsilon_x(x,t)|_{y=d} \\ &= -{\rm i}\frac{a\tau_0(F_1 - F_2)}{\mu} \sum_{\xi^{\rm s}} \frac{\sin(\xi^{\rm s} a) N_{\rm s}(\xi^{\rm s})}{D'_{\rm s}(\xi^{\rm s})} {\rm e}^{{\rm i}(\xi^{\rm s} x - \omega t)} \\ &\quad -{\rm i}\frac{a\tau_0(F_1 + F_2)}{\mu} \sum_{\xi^{\rm a}} \frac{\sin(\xi^{\rm a} a) N_{\rm a}(\xi^{\rm a})}{D'_{\rm a}(\xi^{\rm s})} {\rm e}^{{\rm i}(\xi^{\rm a} x - \omega t)}, \end{aligned} \tag{3}$$

where $F_1(\omega)$ and $F_2(\omega)$ are the Fourier transforms of $f_1(t)$ and $f_2(t)$ and are abbreviated by F_1 and F_2, respectively, $\xi^{\rm s}$ and $\xi^{\rm a}$ are the Lamb wave wavenumbers corresponding to the symmetric and the antisymmetric cases, respectively. The $N_{\rm s}$, $N_{\rm a}$, $D_{\rm s}$ and $D_{\rm a}$ are given as

$$\begin{aligned} N_{\rm s} &= \xi q(\xi^2 + q^2)\cos(pd)\cos(qd), \\ N_{\rm a} &= \xi q(\xi^2 + q^2)\sin(pd)\sin(qd), \\ D_{\rm s} &= (\xi^2 - q^2)^2 \cos(pd)\sin(qd) \\ &\quad + 4\xi^2 pq \sin(pd)\cos(qd), \\ D_{\rm a} &= (\xi^2 - q^2)^2 \sin(pd)\cos(qd) \\ &\quad + 4\xi^2 pq \cos(pd)\sin(qd), \end{aligned} \tag{4}$$

where $\xi = \omega/c$, $p^2 = \frac{\omega^2}{c_{\rm l}^2} - \xi^2$, and $q^2 = \frac{\omega^2}{c_{\rm t}^2} - \xi^2$.

For the case of circle actuator excitation, the stain wave solution of the Lamb wave equation is obtained in the cylindrical coordination system. The boundary conditions in this case become

$$\begin{cases} \sigma_{zz}|_{z=\pm d} = 0, & |r| < \infty, \\ \sigma_{zr}|_{z=d} = \tau(r) f_1(t), & |r| < a, \\ \sigma_{zr}|_{z=-d} = \tau(r) f_2(t), & |r| < a, \end{cases} \tag{5}$$

where $\tau(r) = a\tau_0 [\delta(r-a)]$, with a being the radius of the actuator. The result shown in Eq. (3) can be extended to the case of circle actuator excitation, in which the Bessel and the Hankel functions instead of the sine and the exponential functions appear in the stain wave solution.[14] The corresponding expression based on the Bessel function is derived to be

$$\begin{aligned} &\varepsilon_r(r,t)|_{z=d} \\ &= -\pi{\rm i}\frac{a\tau_0(F_1 - F_2)}{\mu} {\rm e}^{{\rm i}\omega t} \sum_{\xi^{\rm s}} \frac{{\rm J}_1(\xi^{\rm s} a) N_{\rm s}(\xi^{\rm s})}{D'_{\rm s}(\xi^{\rm s})} \\ &\quad \times \left[\xi^{\rm s} {\rm H}_0^{(2)}(\xi^{\rm s} r) - \frac{1}{r}{\rm H}_1^{(2)}(\xi^{\rm s} r) \right] \\ &\quad -\pi{\rm i}\frac{a\tau_0(F_1 + F_2)}{\mu} {\rm e}^{{\rm i}\omega t} \sum_{\xi^{\rm a}} \frac{{\rm J}_1(\xi^{\rm a} a) N_{\rm a}(\xi^{\rm a})}{D'_{\rm a}(\xi^{\rm a})} \\ &\quad \times \left[\xi^{\rm a} {\rm H}_0^{(2)}(\xi^{\rm a} r) - \frac{1}{r}{\rm H}_1^{(2)}(\xi^{\rm a} r) \right], \end{aligned} \tag{6}$$

where $\rm J_1$ is the Bessel function of the first kind and order unity, $\rm H_0^{(2)}$ and $\rm H_1^{(2)}$ are the complex Hankel functions of the second type and orders zero and unity, respectively. Xu and Giurgiutiu[11] have demonstrated that the normalized strain curves and the corresponding measured voltage follow the general sine function and can be used as a theoretical model to predict the excitation frequency of the single mode Lamb wave. Therefore, in subsequent analytical and numerical computations, we adopt the stain wave solutions to replace the voltage outputs of the Lamb waves. We apply the same transient voltage excitation signals to both actuators, i.e., $f_1(t) = f_2(t)$ and, therefore, $F_1(\omega) = F_2(\omega)$. If the action directions of $f_1(t)$ and $f_2(t)$ are the ones shown in Fig. 1(a), i.e., the top and the bottom actuators are excited in an antisymmetric manner, then formulas (3) and (6) contain only pure antisymmetric modes. If the action directions of $f_1(t)$ and $f_2(t)$ are the ones shown in Fig. 1(b), i.e., the two actuators are excited symmetrically, then formulas (3)

and (6) contain only pure symmetric modes. If only the top actuator is excited, as shown in Fig. 1(c), then formulas (3) and (6) contain both the symmetric and the antisymmetric modes.

3. Numerical verification

The Lamb wave excited and sensed by the piezoelectric transducers is studied using the finite element method with ANSYS. The investigation is carried on a simple one-dimensional model of an aluminum specimen with dimensions of 2800 mm in length and 3.2 mm in thickness. The density and the elastic constants of the aluminum plate used in the analytical and numerical calculations are $\rho = 2700$ kg/m^3, $E = 7.1 \times 10^{10}$ N/m^2, and $v = 0.33$. Rectangular and circle actuators A and B with a length of 7 mm are bonded on both free surfaces of the plate. Sensor C is 500 mm away from the actuators, as illustrated in Fig. 2. The distance is designed so that the reflections from the boundaries would not interfere with the first transmitted pulse received by the sensor over the frequency range. The design is based on the theoretical group velocity dispersion for the aluminum plate shown in Fig. 3. The three piezoelectric transducers are of the same material and the material properties are described by[15]

$$\begin{bmatrix} T_1 \\ T_2 \\ T_3 \\ T_{23} \\ T_{13} \\ T_{12} \end{bmatrix} = \begin{bmatrix} 14.2 & 9.19 & 10.2 & 0 & 0 & 0 \\ 9.19 & 14.2 & 10.2 & 0 & 0 & 0 \\ 10.2 & 10.2 & 14.1 & 0 & 0 & 0 \\ 0 & 0 & 0 & 2.55 & 0 & 0 \\ 0 & 0 & 0 & 0 & 2.55 & 0 \\ 0 & 0 & 0 & 0 & 0 & 2.51 \end{bmatrix} \begin{bmatrix} S_1 \\ S_2 \\ S_3 \\ S_{23} \\ S_{13} \\ S_{12} \end{bmatrix} \cdot 10^{10} - \begin{bmatrix} 0 & 0 & -11.7 \\ 0 & 0 & -11.7 \\ 0 & 0 & 19.7 \\ 0 & 14.3 & 0 \\ 14.3 & 0 & 0 \\ 0 & 0 & 0 \end{bmatrix} \begin{bmatrix} E_1 \\ E_2 \\ E_3 \end{bmatrix},$$

$$\begin{bmatrix} D_1 \\ D_2 \\ D_3 \end{bmatrix} = \begin{bmatrix} 0 & 0 & 0 & 0 & 14.3 & 0 \\ 0 & 0 & 0 & 14.3 & 0 & 0 \\ -11.7 & -11.7 & 19.7 & 0 & 0 & 0 \end{bmatrix} \begin{bmatrix} S_1 \\ S_2 \\ S_3 \\ S_{23} \\ S_{13} \\ S_{12} \end{bmatrix} + \begin{bmatrix} 1514 & 0 & 0 \\ 0 & 1514 & 0 \\ 0 & 0 & 1299 \end{bmatrix} \varepsilon_0 \begin{bmatrix} E_1 \\ E_2 \\ E_3 \end{bmatrix},$$

where T is the stress in units of Pa, E is the electric field in units of V/m, D is the electric displacement in units of C/m^2, S is the strain, ε_0 is the dielectric permittivity of the free space. For a sheet of piezoelectric material, the poling direction along the thickness is denoted as the 3-axis, and the 1- and the 2-axes are in the plane of the sheet. The excitation signal is a Hanning window smoothed tone burst in the form of

$$f(t) = 0.5\left[1 - \cos(2\pi t/T_{\rm H})\right], \quad t \in [0, T_{\rm H}], \qquad (7)$$

where $T_{\rm H} = N_{\rm b}/f$, with $N_{\rm b}$ being the burst count and f is the central frequency of the excitation signal.

In the numerical simulation, the Lamb waves are generated by applying pin forces to the nodes located at the ends of the actuators in the condition of ideal bonding. The theory presented in Section 1 has illuminated that the pure symmetric Lamb wave modes are excited by exerting in-phase pin forces to the top and he bottom surfaces, the pure antisymmetric Lamb wave modes are excited by applying out-of-phase pin forces, and the hybrid Lamb wave modes are excited by only exerting pin force to the top or the bottom surface.

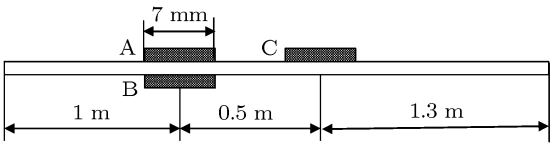


Fig. 2. Aluminum plate model with two pairs of surface-bonded PZT actuators to generate pure Lamb wave modes

We first consider the case in which the signal is excited using a rectangular transducer. The excitation signal is a 5-cycle sine signal with a centre frequency of 50 kHz modulated by the Hanning window. The results are obtained analytically and numerically, and

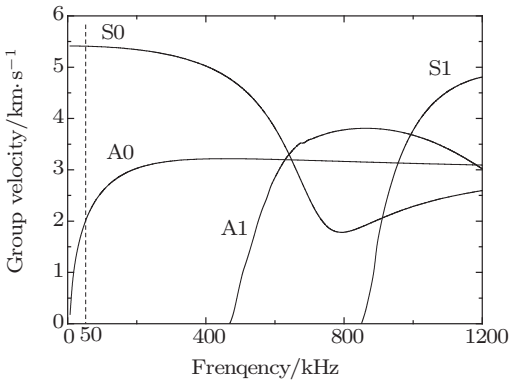


Fig. 3. Group velocity dispersion curve for a 3.2 mm-thick aluminum plate.

are shown in Fig. 4. It can be seen that the main wave packet results are in very good agreement with each other. It is worth mentioning that the boundary reflection appears only in the numerical simulation, as no boundary exists in the wave propagation direction in the analytical model. In Fig. 4(b), the second and third wave packets are the S0 modes reflected from the left and right boundaries of the plate, respectively. Their arrival times are close to the estimated ones (462 μs and 573 μs) based on the theoretical group velocity (5410 m/s) of the S0 mode at 50 kHz. Similarly, the analytical and numerical solutions excited using the circle actuators are also obtained,

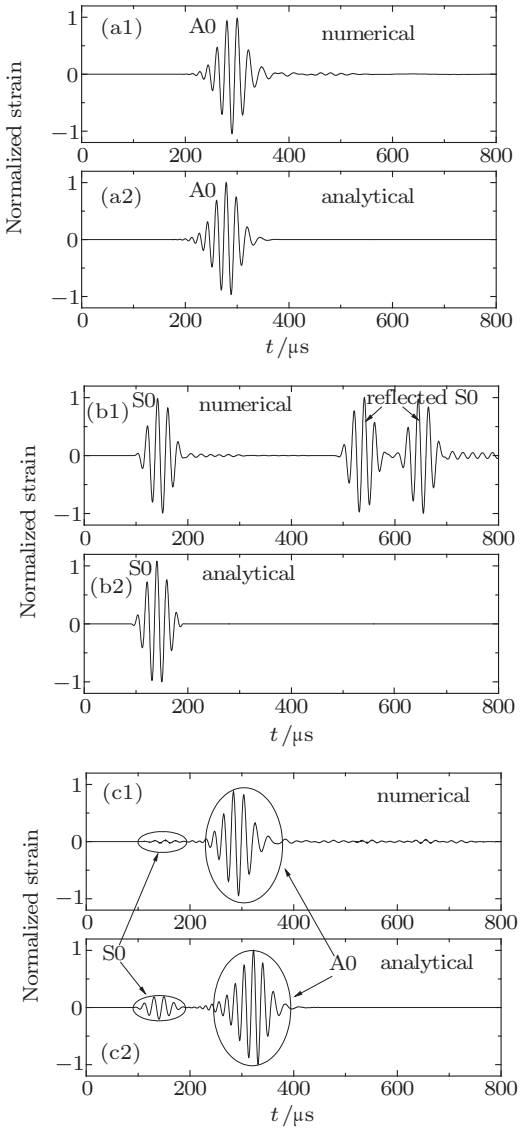


Fig. 4. Numerical and analytical solutions with an appropriate centre frequency of 50 kHz excitation using rectangular actuators. Panels (a1) and (a2) give the solutions for the A0 mode, panels (b1) and (b2) for the S0 mode, and panels (c1) and (c2) for mixed S0 and A0 modes.

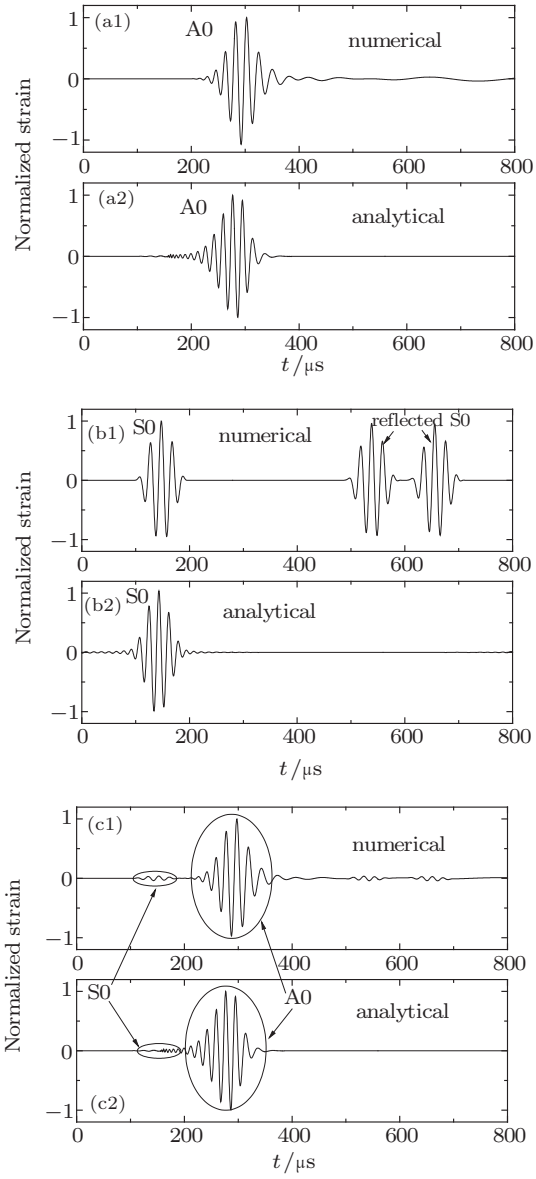


Fig. 5. Numerical and analytical solutions with a centre frequency of 50 kHz excitation using circle actuators. Panels (a1) and (a2) give the solutions for the A0 mode, panels (b1) and (b2) for the S0 mode, and panels (c1) and (c2) for mixed S0 and A0 modes.

as shown in Fig. 5. It can be seen that the analytical and numerical solutions match each other very well, regardless of whether one pure mode is excited or two modes are excited simultaneously. In Figs. 4(c) and 5(c), because the amplitude of the S0 mode is much smaller than that of the A0 mode, the reflected boundary amplitudes of the S0 mode are too small to be observed.

4. Parameter selection

Pure A0 or S0 mode excitation can be achieved by using two actuators located separately on the top and the bottom surfaces of the structure. However, the strictly symmetric qualification of the two actuators must be met, which sets a high requirement for the experimental system. As observed in Figs. 4(c) and 5(c), the single mode can also be excited by using a single actuator with a central frequency, for which the peak wave amplitude ratio between S0 and A0 modes is the maximum.[13] In Eqs. (3) and (6), the $\sin(\xi a)$ and the $J_1(\xi a)$ terms change according to the sine rule and present maximum and minimum values at some frequencies. These frequencies are related to the transducer's geometric shape and length.

Figures 6 and 7 show the S0 and the A0 Lamb wave responses calculated using Eqs. (3) and (6) under rectangular and circlar PZT excitations with sizes of 26 mm and 43 mm, respectively. It can be seen that the strain wave amplitude changes faster with the frequency for the larger PZT. The effect of the PZT shape on extremum position is demonstrated in the two figures. As shown in Fig. 6(a), for the 26 mm rectangular PZT excitation, the S0 mode is larger, while the A0 mode is smaller at 255 kHz. At a similar excitation frequency of 250 kHz for the 26 mm circle PZT excitation, the A0 mode is larger, while the S0 mode is smaller, as shown in Fig. 7(a). The extremum position is also affected by the PZT length. For example, the 26 mm circular PZT generates a larger S0 mode at 150 kHz, while the 43 mm circle PZT generates a larger A0 mode at a similar excitation frequency of 152 kHz, as shown in Figs. 7(a) and 7(b).

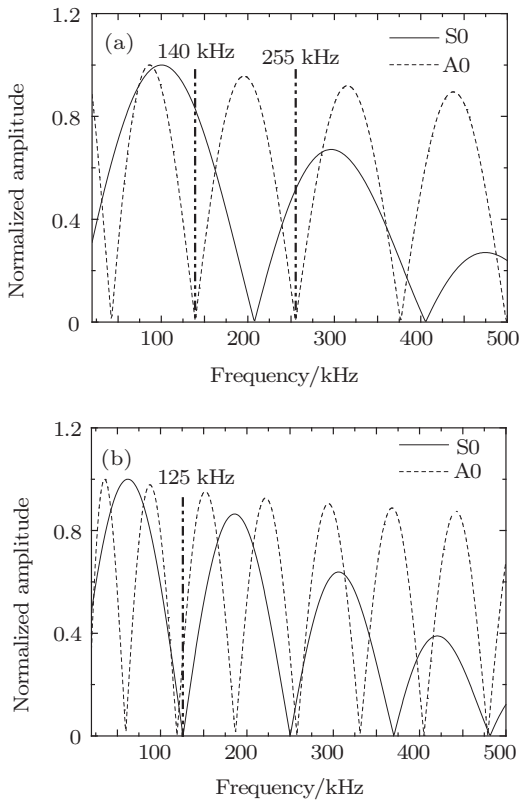


Fig. 6. The S0 and A0 Lamb wave responses versus frequency under rectangular PZT excitation with lengths of 26 mm (a) and 43 mm (b), respectively.

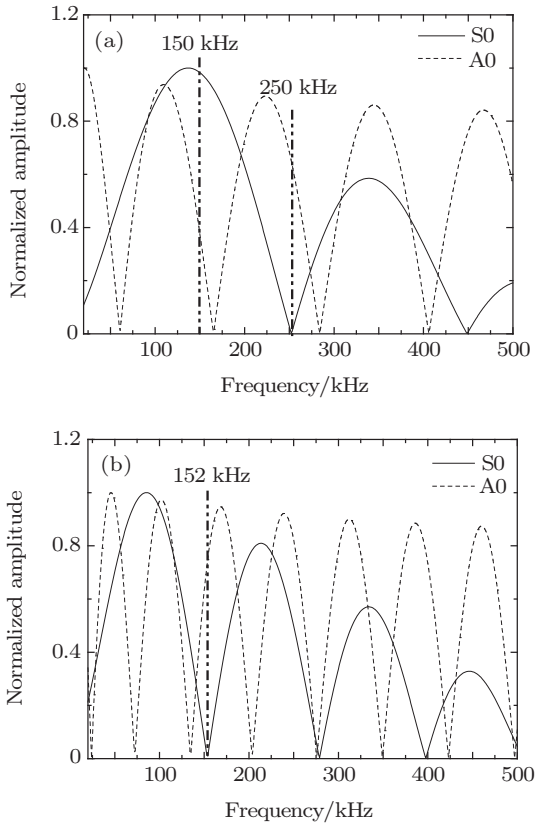


Fig. 7. The S0 and A0 Lamb wave responses versus frequency under circular PZT excitation with lengths of 26 mm (a) and 43 mm (b), respectively.

An experiment is also carried out to study the effect of the PZT shape, length and excitation frequency on the Lamb wave output waveform. The set

up consists of a tone-burst ultrasonic pulser for the signal generation, a digital oscilloscope for the signal acquisition, and a pair of PZTs for the excitation and reception of the Lamb wave. An aluminum plate with dimensions of 1000 mm×1000 mm×3.2 mm is used. The input is a 5-cycle tone burst fed to transmitting PZT A. Receiving PZT B has the same properties and length as transmitting PZT A, and sits 0.5 m away from PZT A. The transducer layout is schematically shown in Fig. 8.

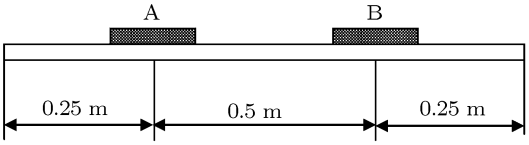


Fig. 8. Experimental layout of transmitting PZT A and receiving PZT B.

Figure 9 shows the experimental Lamb wave outputs of PZT B using transmitting PZT A with different shapes, lengths and excitation frequencies. In these waveforms, the three forward wave packets are S0, A0 and reflected S0 modes from left to right, respectively. As shown in Fig. 9, the S0 mode is larger and the A0 mode is smaller under 26 mm rectangular PZT excitation with the central frequencies of 140 kHz and 150 kHz. While the S0 mode is smaller and the A0 mode is larger under 43 mm circular PZT excitation with central frequencies of 125 kHz and 150 kHz. The relative amplitudes of the S0 and A0 modes are in agreement with the numerical strain wave amplitudes of these two modes shown in Figs. 6 and 7. It can also be seen from Figs. 9(c) and 9(d), at the same excitation frequency of 150 kHz, that the 26 mm rectangular and the 43 mm circle PZTs generate different Lamb waveforms. If we want to generate the S0 mode, the 26 mm rectangular PZT should be selected. We should select the 43 mm circle transducer to generate the A0 mode.

The analysis results of Fig. 9 are verified by the group velocity calculations of the S0 and A0 modes using the formulas $V_{\mathrm{gS0}} = l_{\mathrm{AB}}/\Delta t_1$ and $V_{\mathrm{gA0}} = l_{\mathrm{AB}}/\Delta t_2$, respectively, where l_{AB} is the distance between transmitting PZT A and receiving PZT B, Δt_1 and Δt_2 are the time differences between S0 and the exciting signal envelope peaks, and between A0 and the exciting signal envelope peaks, respectively, as demonstrated in Fig. 10. Table 1 shows the calculated results of the S0 and the A0 group velocities for four cases shown in Fig. 9, which are approximately equal to the theoretical velocities shown in Fig. 3.

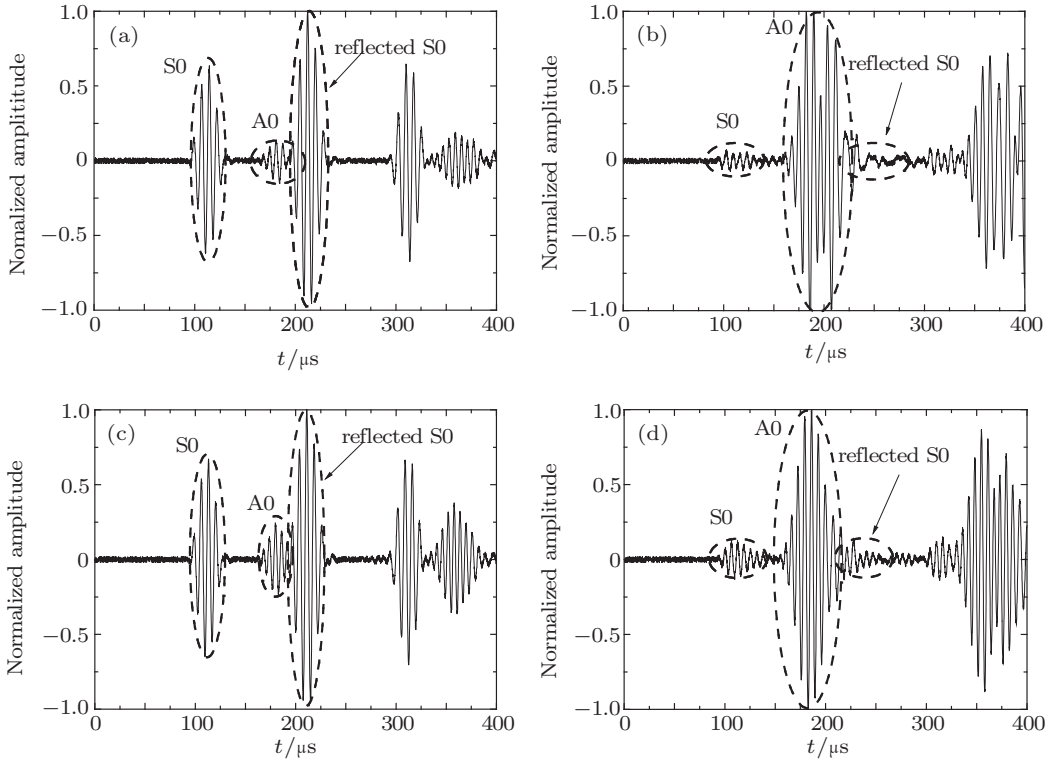


Fig. 9. Experimental Lamb wave outputs of PZT B using transmitting PZT A with different excitation frequencies, shapes and sizes. (a) 26 mm rectangular transducer with a centre frequency of 140 kHz. (b) 43 mm round transducer with a centre frequency of 125 kHz. (c) 26 mm rectangular transducer with a centre frequency of 150 kHz. (d) 43 mm round transducer with a centre frequency of 150 kHz.

Table 1. Calculation results of S0 and A0 group velocities for four cases shown in Fig. 9.

Mode	S0				A0			
Frequency/kHz	Δt_1 /μs	Calculated / m·s^{-1}	Theoretical / m·s^{-1}	Error / m·s^{-1}	Δt_2 /μs	Calculated /m·s^{-1}	Theoretical / m·s^{-1}	Error / m·s^{-1}
140[a)]	95.1	5260	5381.8	0.0226	163.9	3050	2815.8	0.0832
150[a)]	95.8	5220	5375.3	0.0289	165	3030	2871.99	0.0550
125[b)]	84.6	5910	5387	0.0971	165.7	3020	2815.8	0.0725
150[b)]	93.1	5370	5375.3	0.0009	166.9	3000	2871.99	0.0446

[a)] $2a = 26$ mm rectangular PTZ, [b)] $2a = 43$ mm round PZT.

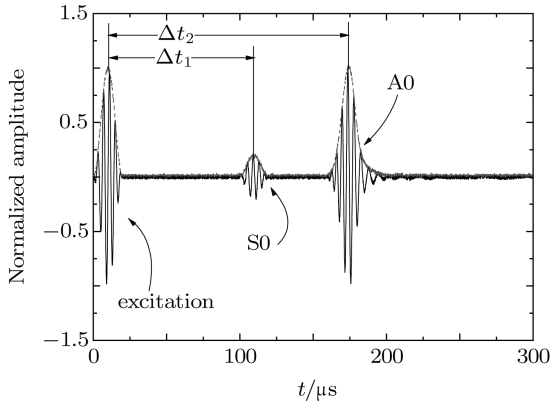


Fig. 10. Arrival time calculations of the S0 and the A0 modes.

5. Conclusion

Due to their small size, low cost and easy bonding to structures, piezoelectric transducers have been widely used for transmitting and receiving Lamb waves. Considering the coupling effect between the piezoelectric transducer and the plate, we investigate the excitation and the propagation of Lamb waves using rectangular and circular piezoelectric transducers surface-bonded to an isotropic plate. Analytical stain wave solutions for the Lamb wave fields are respectively derived for the two transducer shapes. The analytical study is supported by numerical analysis using the finite element method and experimental investigation. The conclusions are as follows.

(i) The combination of the Lamb wave approach and the piezoelectric transducers can offer an alterative Lamb wave detection system that is capable of selectively generating symmetrical, antisymmetrical and mixed modes. Since the mode selection is one of the advantages of the Lamb wave detection, this method can improve the sensitivity of defect detection.

(ii) We can excite pure A0 or S0 modes by symmetrically locating transducers on the top and bottom surfaces of the plate (double side excitation). It should be noted that the requirements for such an experimental system is higher. The two piezoelectric wafers acting as actuators must maintain high consistency in the coupled location and extent of the structure. In addition, compared with the single side excitation method in which only one actuator is used, the double excitation method demands double the transducer numbers, which increases the hardware requirement accordingly.

(iii) By placing the piezoeletric transducer only on the top or bottom surface of the plate and weakening the strength of one mode while enhancing the strength of the other modes to find the centre frequency, with which the peak wave amplitude ratio between the S0 and A0 modes is maximum, we can also approximately excite a single mode from the multiple modes of Lamb waves. However, system parameters, such as the transducer shape, length and central frequency, must be considered comprehensively.

It should be noted that this research work is carried out on a health structure. The combination of the Lamb wave approach and the optimal transducer parameters, such as shape, length and central frequency, to detect a damaged structure will be carried out in the next work.

References

[1] Lu Y, Wang X, Tang J and Ding Y 2008 *Smart Mater. Struct.* **17** 025034

[2] Li F C and Meng G 2008 *Acta Phys. Sin.* **57** 4265 (in Chinese)

[3] Zhang H Y, Liu Z Q and Ma X S 2003 *Acta Phys. Sin.* **52** 2492 (in Chinese)

[4] Xiang Y X and Deng M X 2008 *Chin. Phys.* B **17** 4232

[5] Zhu X F, Liu S C, Xu T, Wang T H and Cheng J C 2010 *Chin. Phys.* B **19** 044301

[6] Zhang H Y, Sun X L, Cao Y P, Chen X H and Yu J B 2010 *Acta Phys. Sin.* **59** 7111 (in Chinese)

[7] Zhang H Y, Chen X H, Cao Y P and Yu J B 2010 *Chin. Phys. Lett.* **27** 104301
[8] Yu L, Santoni G B, Xu B, Liu W and Giurgiutiu V 2008 *Fatigue Fract. Eng. M.* **31** 611
[9] Giurgiutiu V, Bao J and Zhao W 2003 *Exp. Mech.* **43** 428
[10] Lin X and Yuan F G 2001 *Smart Mater. Struct.* **10** 907
[11] Xu B and Giurgiutiu V 2007 *J. Nondestruct Eval.* **26** 123
[12] Santoni G B, Yu L, Xu B and Giurgiutiu V 2007 *J. Vib. Acoust.* **129** 752
[13] Wang X, Lu Y and Tang J 2008 *Smart Mater. Struct.* **17** 025033
[14] Raghavan A and Cesnik E S C 2005 *Smart Mater. Struct.* **14** 1448
[15] Nieuwenhuis J H, Neumann J, Greve D W and Oppenheim I J 2005 *IEEE Trans. Ultrason. Ferroelet. Freq. Control* **52** 2103